Quantifying the effects of climate change, carbon fertilization and modern sample bias in boreal jack pine (*Pinus banksiana*) forests

Jacob Cecile[1], F. Wayne Bell[2], Lucas Silva[3], William Horwarth[3], Madhur Anand[1]

Abstract

Climate change and increasing atmospheric carbon dioxide levels are thought to be responsible for recent shifts in global forest growth. Tree ring chronologies are a crucial tool for identifying and understanding these changes, but their use for reliably reconstructing long-term trends in growth is hampered by the presence of modern sample bias.

Using fixed effects standardization, we demonstrate and correct modern sample bias in a young living jack pine (*Pinus banksiana* Lamb.) chronology from northwestern Ontario, Canada, by accounting for tree-level productivity. The choice of standardization model had a pronounced effect on the estimated underlying trend in tree growth over time (1879-2010). The long-term trend of growth was generally flat, suggesting that the combined effects of climate change and carbon fertilization has been fairly neutral for the jack pine studied.

This corrected chronology was sensitive to June temperatures, late winter precipitation and growing season length. Growth followed a concave down relationship with growing degree days, a signal that was completely missed by linear response functions. Rising levels of atmospheric carbon dioxide (CO_2) substantially increased water use efficiency (computed from whole-wood $\delta^{13}C$), which showed a nonlinear relationship to growth. At low levels of water use efficiency, increases resulted in increased growth, as would be expected if water availability is constant. But at higher levels, growth declined with increases in water use-efficiency, suggesting that it also acts as an indicator of drought, increasing as trees close their stomata.

Keywords: fixed effects standardization, $\delta^{13}C$, climate response, dendrochronology, water use efficiency, non-linearity

1. Introduction

Since the industrial revolution, a shifting climate and increasing carbon dioxide (CO_2) levels have disrupted patterns of forest growth [*Newman et al.*, 2011]. Evidence for a positive effect of CO_2 on forest growth, often referred to as "carbon fertilization", is mixed and controversial. Laboratory experiments and theoretical expectations show that tree growth increases due to improved photosynthetic efficiency and decreased in stomatal conductance, which reduce water requirements [*Conroy et al.*, 1986; *Huang et al.*, 2007]. But as CO_2 levels increase other developmental and ecological changes occur, making it difficult to extrapolate these results to a

more natural setting, [*Asshoff et al.*, 2006; *Stewart and Hoddinott*, 1993]. As a result, outdoor large-scale Free Air Carbon dioxide Enrichment (FACE) experiments have been set up to examine the effects of carbon fertilization[*Asshoff et al.*, 2006; *Körner et al.*, 2005; *Norby et al.*, 2005]. Reviews of the findings suggest that direct CO_2 enrichment typically increases tree productivity but these gains are often slowed as other factors (typically nutrients, with nitrogen being the most studied) become more limiting; plant species composition may also shift [*Ainsworth and Long*, 2005; *Norby and Zak*, 2011].

Tree rings can serve as a record of tree growth long into the past, and are a powerful tool for understanding the link between growth and the environment. Attempts to find evidence for carbon fertilization in the tree ring records suffer from several methodological difficulties, but recent global analyses suggests that the effect is largely absent [*Gedalof and Berg*, 2010; *Peñuelas et al.*, 2011; *Silva and Anand,* 2012].The primary challenge in dendrochronological analysis is the extraction of a reliable index of tree growth over time (or alternate measurements such as wood isotope ratios). The analysis of tree ring data cannot be divorced from its fundamentally ecological context; growth varies not only by year but with age and species and microsite as well. To address this, dendrochronologists turn to the techniques of standardization, controlling for unwanted effects (typically age-driven) to extract a common, climate-sensitive chronology. The two broad approaches to this problem are individual series standardization and regional curve standardization. Individual series standardization is intended to remove the age-driven trend in one series (a tree ring record from a single tree) at a time, using parametric models of the change in growth by age or by removing low-frequency (presumably age-driven) variability. As a result, individual series standardization is a poor approach for capturing long-term trends in growth [*Cook et al.*, 1995]. In contrast, regional curve standardization is used to estimate the common effect of age on each tree, remove it, and then estimate the time-driven variability (referred to as forcing) [*Briffa and Melvin*, 2011].

If, however, the observed tree ring data varies systematically by tree as well, the estimates produced by regional curve standardization are flawed. This is known as differing-contemporaneous-growth-rate bias, and when the link between tree productivity and either age or year is persistent, it results in modern sample bias [*Briffa and Melvin*, 2011]. In that case, the time signal is underestimated in years where the mean intrinsic growth rate of the trees in the chronology is low, and overestimated where it is high. The high frequency variability is retained accurately, but the long-term trend is compromised, making the detection of carbon fertilization or climate change effects extremely difficult [*Brienen et al.*, 2012a,b]. Fixed effects standardization extends regional curve standardization using classical regression techniques to account for tree-level productivity as well, providing a simple solution to the problem of modern sample bias [*Cecile et al.*, in review].

Once a time signal is extracted, the major challenge is to show that the increasing atmospheric CO_2 levels are positively affecting tree growth. Merely showing that tree growth is increasing [c.f. *LaMarche et al.,* 1984] is not sufficient; investigators need to control for other important environmental changes, especially climate [*Gedalof and Berg*, 2010; *Jacoby*, 1997].

We investigate these questions in the context of a homogeneous chronosequence of even-aged jack pine (*Pinus banksiana* Lamb.) stands in northwestern Ontario. Ring-width measurements provided

the central evidence for changes in tree growth from 1879-2010 while carbon isotope ratios ($\delta^{13}C$, or ^{13}C:^{12}C) were used to reconstruct water use efficiency. Traditional bootstrapped linear response functions and generalized additive models were used to model the links between climate, water use efficiency and growth.

2. Methods

2.1 Site description

Nineteen even-aged jack pine stands ranging in stand establishment dates from 1872-1999 (by date of pith emergence) in a 30 km radius near Silver Dollar, Ontario were studied (approximately centred around 49° 50' N, 91° 18' W) (Figure 1). Fifteen of the sites originated from stand-replacing fire, while four developed after a clearcut harvest. These sites are since undisturbed and unmanaged, with the exception of one harvest-origin site established in 1980 and thinned in 2008-2009. This relatively remote location in Northwestern Ontario helps reduce the effect of simultaneous anthropogenic changes in short- to medium range atmospheric pollutants, particularly NO_x, SO_2, ozone, and particulates that have been shown to have significant effects on tree growth and nutrient cycling [*Dietze and Moorcroft*, 2011]. All stands were jack pine dominated, with many of the older stands containing younger *Populus spp.* (poplar), *Abies balsamea* (balsam fir), *Picea mariana* (black spruce) or *Picea glauca* (white spruce) in the understory. The soil on all sites was a deep (>50 cm) OrthicHumo-Ferric Podzol[*SCWG*, 1998]. For the fire-origin sites, all Ae and Bf horizons were coarse sand, silty sand, or loamy sand (mean percent sand, silt, clay was 84.4±8.3, 11.5±7.8, 4.1±1.6, respectively) and mean pH was 5.4 ± 0.2 while the LFH layer was thin (1 to 2 cm) on all sites. Detailed soil data was not available for the remaining four harvest origin sites.

2.2 Climate data

Monthly interpolated climate data for a single centrally located point at 49.849915° N, 91.304131° W for the period 1901 to 2007 were obtained from Canadian Forest Service using the model outlined in *McKenney et al.* [2006]. The study sites had a mean annual precipitation of 690 mm per year, a mean annual temperature 1 °C, and typically experience a 165-day growing season. Rainfall is strongly seasonal, with about 65% occurring during the growing season. July is typically the hottest month of the summer, while August is the driest, so drought may occur during the growing season.

2.3 Species description

Jack pine is a short-lived, shade-intolerant pioneer species native to eastern and central boreal forests, with a range extending south to surround lakes Superior, Michigan, and Huron [*Rudolph and Laidly*, 1990]. Through the use of common garden trials, Thomson and Parker [2008] showed that the “optimum latitude” for this species is between 46°N and 47°N, slightly south of our study sites. Jack pine is frequently found on xeric, well-drained sites but grows faster in mesic conditions and is considered relatively drought tolerant [*Rudolph and Laidly*, 1990].

2.4 Sampling and chronology preparation

At each of the 19 sites, 10 dominant/codominant canopy trees were sampled at 25 m intervals along a linear transect, offsetting then doubling back if stand boundaries were reached. In July 2011, two perpendicular cores per tree were taken at 1.3 m above the ground, then sanded, scanned, and measured, taking care to avoid carbon isotope contamination. Cores with intact bark were dated directly; other cores were visually and statistically crossdated against these using t and trend statistics in Corina [*Brewer et al.*, 2010]. The stands were known to be even-aged; to reduce the effect of missing pith years when standardizing the chronology, all series were assumed to originate in the year of stand establishment for the purposes of determining age. The sample depth (number of series included in the chronology) of the chronology is displayed in Figure 2.

2.5 Tree ring width standardization

Fixed effects standardization was used to separate the effects of tree-level productivity, age, and time on ring width and correct for modern sample bias [*Cecile et al.*, in review]. Preliminary examination of the residuals and model fit statistics revealed that the error term was more appropriately treated as log-normal (rather than normal) and the form of the model was multiplicative (rather than additive). As a result, the growth models explored to standardize the chronology were nested models of the following full model:

$$G_{ita} = I_i \cdot T_t \cdot A_a \cdot \epsilon_{ita}^{L}$$

G_{itr} is the observed ring width at tree i, year t, and age a. I, T and A are categorical effects that influence tree growth: I_i is the individual effect and describes the intrinsic productivity of that tree, T_t is the time effect (equivalent to the standardized chronology or ring width index) while A_a is the age effect (equivalent to the regional curve). $\boldsymbol{\varepsilon}^{L}$ is a log-normal noise term, that is independent and identically distributed across all observed data points.

There are four potential standardization models contained within the full growth model listed above. Each of the models includes a time effect (as the goal of the analysis is to observe how tree growth varies by time) and corresponds to a competing traditional technique of tree ring standardization. Throughout the paper, these models are referred to by the list of effects included in the model for brevity (e.g. the full model has the code "ITA").

The first, most obvious model contains only a time effect and is equivalent to the practice of using "raw" ring-width measurements in dendrochronological analysis. This practice can be written as a model:

$$G_{ita} = T_t \cdot \epsilon_{ita}^{L}$$

The second model adds an effect for age, and corresponds to the practice of regional curve standardization [*Briffa et al.*, 1992]. The implementation here however uses a superior optimization algorithm than the traditional sequential estimation of age, then time effects

and is thus free from trend-in-signal bias [*Melvin and Briffa*, 2008]. The regional curve standardization model is:

$$G_{ita} = T_t \cdot A_a \cdot \epsilon^L_{ita}$$

Instead of age, one might propose that the major source of bias is differences in growth rate between contemporaneous trees or cores. In that case, the traditional answer is to use flat detrending, eliminating the persistent differences in growth rates between trees [*Fritts*, 1976]. Flat detrending uses a model that accounts for individual and time effects. The implementation used in this paper is again superior to traditional flat detrending as it uses an unbiased optimization algorithm that can deal with the unavoidably unbalanced design. In algebraic terms, the model is:

$$G_{ita} = I_i \cdot T_t \cdot \epsilon^L_{ita}$$

Combining the three approaches, we can use the full fixed effects standardization model, simultaneously accounting for the effect of individuals, time and age. This allows us to account for common age-signals while avoiding modern sample bias caused by heterogeneity in the productivity of the trees. The post-hoc correction for likelihood ridges in three-effect models detailed in *Cecile et al.* [in review] was used to ensure reliability of the estimated effects. The full model used is:

$$G_{ita} = I_i \cdot T_t \cdot A_a \cdot \epsilon^L_{ita}$$

The estimated effects for each of these standardization models is shown, and the models are compared using goodness of fit statistics. These models can be fit using a variety of different optimization algorithms, for this paper we used the variant of signal-free standardization [*Briffa and Melvin*, 2011; *Melvin and Briffa*, 2008] described in *Cecile et al.* [in review]. For a full theoretical justification of these concepts and their relation to flat detrending, regional curve standardization and signal-free algorithms, the interested reader is referred to *Cecile et al.* [in review].

2.6 Carbon isotope ratios and water use efficiency

Intrinsic water use efficiency (W_i) is the ratio between plant carbon fixation and stomatal conductance and can be approximately determined by the discrimination against ^{13}C [*Farquhar et al.*, 1982]. Because compounds deposited in tree rings have fixed stable isotope ratios, historical records are commonly constructed using one of the various forms of the equation below [*Duquesnay et al.*, 1998], in which C_a is the atmospheric concentration of CO_2, *a* is the diffusion fractionation across the boundary layer and the stomata (≈4.4‰), and *b* is the RuBisCo enzymatic biologic fractionation (≈27.0‰). Δ is defined as the isotopic discrimination, and is simply calculated from δ, the deviation from the PeedeeBelmenite (PDB) carbonate standard as follows:

$$\Delta_{wood} = \frac{(\delta_{atm} - \delta_{wood})}{1000 + \delta_{wood}} \cdot 1000$$

$$W_i = \frac{C_a}{1.6}\left(1 - \frac{\Delta_{wood}}{b - a}\right)$$

Samples from the same site and year were pooled due to cost constraints, providing an increased sensitivity to interannual variation in climate compared to serial or "pentad" pooling at the cost of information about intertree variability [*Leavitt*, 2008, 2010; *Liñán et al.*, 2011]. $\delta^{13}C$ for all the wood samples was determined by the Stable Isotope Facility at University of California Davis using a continuous flow Isotope Ratio Mass Spectrometer. Cellulose extraction was not performed, as studies show little or no accuracy improvement for ^{13}C [*Barbour et al.*, 2001; *English et al.*, 2011].

Changing levels of atmospheric $\delta^{13}C$ were compiled from ice core records as documented by McCarroll and Loader [2004], but extending the linear extrapolation to 2010. Annual atmospheric averages of CO_2 concentration from Mauna Loa, Hawaii (www.esrl.noaa.gov/gmd/ccgg/trends/, courtesy of Dr. Pieter Tans (NOAA/ESRL) and Dr. Ralph Keeling (Scripps Institution of Oceanography)) were supplemented with Lawdome ice core records to construct a historical record of C_a [*Etheridge et al.*, 1998].

Water use efficiency showed strong patterns by year, age, and site. Fixed effects standardization was used, as above, to separate these effects. In contrast to the ring width chronology above, the canonical vectors were scaled such that the magnitude of the data was retained in the time effect (**T**) to aid reader interpretation of typical intrinsic water use efficiency values over time. Additionally, a smooth age effect was assumed using penalized splines and the model was fit using the generalized additive model package *mgcv* [*Wood*, 2006]. Akaike's information criteria confirmed that in this case the full model was most appropriate.

2.7 Links between climate, water use efficiency and growth

The climate sensitivity and responses of jack pine chronologies are well-established in the literature, so we designed our analysis largely to test the previously observed relationships using our data.

Drought-induced growth limitation is a common theme [*Brooks et al.*, 2011; *Girardin et al.,* 2012; *Hoffer and Tardif*, 2009; *Hofgaard et al.*, 1999; *Larsen and MacDonald*, 1995; *Savva et al.*, 2008; *Tardif and Conciatori*, 2001], but warm [*Botkin et al.*, 1991; *Despland and Houle*, 1997; *Hamel et al.*, 2004; *Huang et al.*, 2010] or extended growing seasons have also been found to increase jack pine growth [*Despland and Houle*, 1997; *Hofgaard et al.*, 1999; *Tardif and Conciatori*, 2001]. Growing season growing degree days and growing season precipitation were selected as the drought-linked climate variables as they are fairly general and simple to interpret while growing degree days provided a test for temperature limitation. Growing season length was selected as a largely orthogonal measurement to test the second hypothesis directly. Similarly, previous studies have investigated carbon fertilization in pine [c.f. G*irardin et al.,* 2011; *Nelson* 2012]. Elevated water use efficiency is a compelling mechanistic explanation of this effect so we used the reconstructed typical intrinsic water use efficiency from the $\delta^{13}C$ chronology to investigate it. By examining the response

of ring width to these variables, we could explore the effect of climate change and carbon fertilization on tree growth, while examining the relationship between climate and water use efficiency helped to interpret $\delta^{13}C$ measurements.

We then checked for unexpected climate signals and tested the robustness of the climate response to changes in standardization model by computing bootstrapped linear climate responses using the *bootRes* package in R [*Biondi and Waikul*, 2004]. The season analyzed spanned from February to October of the year of growth, to capture both growing season drivers and the potential effects of stored precipitation or winter damage.

This exploratory analysis suggested that there was a positive response to February and March precipitation and a negative response to June minimum and maximum temperatures. The February and March precipitation data suggested a common mechanism, so they were pooled together as "winter precipitation" (there was no response to December or January precipitation). June minimum and maximum temperatures also indicated a common signal (drought stress) but were highly correlated. June maximum temperature was selected as a predictor variable over minimum temperature due to a slightly stronger response but this decision was mostly arbitrary.

Three other predictor variables were included at the suggestion of the literature and ecological background knowledge. These were deliberately as broad as possible, to avoid cherrypicking for poor or strong responses. They are: summer precipitation (total precipitation during period 3, the growing season), growing degree days and growing season length.

The final predictor variable, water use efficiency, is an attempt to test, mechanistically for potential carbon fertilization effects. Carbon dioxide levels themselves are an extraordinarily inappropriate predictor of growth in this case due to their smooth and monotonic nature. With only one time series to calibrate against, carbon dioxide levels effectively play the role of a latent time variable, absorbing low-frequency trends in growth (especially for generalized additive models, where linearity is no longer required). Instead, water use efficiency, which is itself driven by changes in atmospheric carbon dioxide, is both rougher and more mechanistic. As carbon dioxide levels rise, water use efficiency increases. Increased water use efficiency is a major proposed mechanism for carbon fertilization effects. If this is the case in real ecosystems, we should see a positive relationship between water use efficiency and growth on an inter-annual and decadal scale.

In dendrochronology, it is common practice to assume a linear relationship between tree growth and climate [*Biondi and Waikul*, 2004]. This simplifies analysis and interpretation considerably, especially when the final goal is climate reconstruction, and may be a good assumption when the observed range of variability is small or far from local optima [*Loehle*, 2009]. Nevertheless, nonlinear responses have been shown in tree-ring chronologies [*D'Arrigo*, 2004; *Graumlich and Brubaker*, 1986; *Helama et al.*, 2009; *Ni et al.*, 2002]. Agronomic, ecological, and physiological evidence argue for a nonlinear response to almost all environmental variables, at least over large ranges. Resource demands (CO_2, water, nutrients) can be met but response to temperature is typically hump-shaped: when it is too low the rate of growth and metabolism is reduced and when it is too high drought ensues. To test for these effects, we used both generalized additive models (via thin-plate kernel regression smoothing with the R package *mgcv*, *Wood* [2006]), which assumed

only a locally smooth additive fit, and traditional multivariate linear regression. The standardized ring-width chronology (time effect) was log-transformed to stabilize the variance (the error structure is retained from the original growth model) before fitting climate-growth models.

3. Results

3.1 Tree ring width standardization

Fixed effects standardization splits the ring-width chronology into three components: the individual effect (due to differences in tree-level productivity), the time effect (driven by factors like climate or carbon fertilization), and the age effect (as a result of allometric, ontogenical or stand dynamical influences) (Figure 3). These plots show the estimated effects produced by each of the four competing standardization models.

The three-effect model (ITA) was by a large margin superior to every other other candidate standardization model by every model fit statistic examined (Table 1). The next best model was the flat detrending inspired model (IT), followed by the regional curve standardization inspired model (TA) and finally the "raw" model (T). The remainder of this section refers to results obtained using the superior three-effect model (ITA) unless otherwise noted.

Individual effects (**I**) were roughly log-normal and fairly strong (Figure 1), leading to observed growth values that were between 0.39 and 5.83 times the otherwise expected value. Most observed individual effects were more modest however, with an interquartile range of 0.74-1.34. Individual effects were modestly negatively correlated with age (Spearman's $\rho = -0.45$, $p < 0.01$). This leads, as the next paragraphs show, to a slow-grower-survivorship bias type of modern sample bias.

The age effect (**A**) was quite similar between the two models that included it (ITA and TA). There is a short period of increase (up until about 10 years after stand establishment), followed by an almost exponential decline in growth, and an eventual plateau. The final uptick observed is an artifact of the extremely small sample depth (<5 series) in the chronology for that age. The first section of growth likely corresponds to the initial, free-to-grow portion of the jack pine life cycle, ended by canopy closure. After that, the effects of increasing competition and allometric limitation cause a sharp drop-off in expected ring-width increment per year. The estimated age effect is quite smooth, despite the fact that it was estimated categorically, with no smoothing (post-hoc or via generalized additive models) applied, indicating a strong and predictable pattern of growth by age for these trees.

The high frequency variability between the time effects (**T**) competing standardization models is mostly the same, but the low-frequency variability differs wildly (Figure 3). The raw model (T) suggests no significant long term trend in growth (Spearman's $\rho = -0.06$, $p = 0.50$), the regional curve standardization model (TA) records a strong, highly significant positive trend in growth (Spearman's $\rho = 0.63$, $p < 0.01$), the flat detrending model (IT) indicates an extremely strong, highly significant negative trend in growth (Spearman's $\rho = -0.87$, $p < 0.01$) while the full model (ITA)

again concludes that there is no significant long-term trend in growth (Spearman's $\rho = 0.06$, $p = 0.461$)!

Clearly these interpretations are incompatible, but which model offers a reliable estimate of the true time effects? Model fit (and ecological intuition) suggest that the full model (ITA) offers the most reliable signal, but with a little detective work we can determine how and why the other approaches diverge. We can investigate the impact of adding an effect to the model by comparing the time effect of the models with and without the effect (follow along by examining Figure 3).

In both the T and IT models, there is a steep downward slope from approximately 1870 – 1910. If we move from T to TA, or from IT to ITA, this anomalous section disappears. In addition, the whole chronology becomes slightly more positive in trend. Looking at the age effect and sample depth graph, we see that young trees grow much faster than old or middle-aged trees and that the early section of the chronology is composed almost exclusively of young trees which quickly age. This accounts for the early dramatic decline in the time effect observed for the T and IT models. The fact that tree-growth continues to decline with age results in a small long-term negative bias in time effect when the age effect is omitted, explaining the other half of the observed pattern.,

On the other hand, T and the TA models produce a slightly more positive long-term trend in time effect than the IT or ITA models respectively. Looking at the scatterplot of individual effect by age, we see that individual productivity is negatively correlated with the age of the tree (even after accounting for time- and age-driven changes in growth). This means that the old trees in our chronology are overestimating the effect of time on growth while the young trees are underestimating it. Because the oldest sections of our chronology are composed only of old trees, this results in an underestimate of the time effect in older years and results in a long-term positive bias in growth. This is classical modern sample bias [*Briffa and Melvin*, 2011], which is corrected by adding an estimate of between-tree differences in growth.

The agreement between the models was variable, with the most reasonably good consistency in the estimates of age (**A**) and individual effects (**I**). Examining the correlations of the log-transformed effects (Table 2) confirms this visual intuition. As a result of the long-term biases discussed above, the overall correlation between the models was quite poor, with only the TA standardization model (related to regional curve standardization) performing reasonably well relative to the full ITA model. Alarmingly, the correlation between the time effects estimated by the improved versions of the two most respectable and popular techniques examined (flat detrending, IT, and regional curve standardization, TA) were negatively correlated ($r=-0.448$), leading to completely different pictures of the long-term trend in growth and hence climatic response.

3.2 Water use efficiency

Figure 4 show the effects of intrinsic water use efficiency by stand, year, and age. We can compare the full model to the time-only model (the traditional approach of taking mean values at each year) and see that the model fit is substantially improved, at the cost of extra parameters (Table 3).

Site level effects on water use-efficiency were fairly strong, with an inter-quartile range of 0.74-1.30. The time effect estimated by the two approaches was extremely similar (with a log-Pearson correlation of 0.956), in stark contrast to the impact of standardization on tree ring width data. The time effect water use efficiency increased steadily throughout time due to increasing levels of atmospheric carbon dioxide. Heteroscedasticity is evident in the early section of the chronology due to extremely low sample replication (limited by the number of available old sites). Water use efficiency appears to increase as the trees age, but the details of the age effect are hard to make out due to a weak signal and poor replication.

3.3 Links between climate, growth and water use efficiency

As an exploratory analysis, we checked bootstrapped climate responses of each estimated time effect (depending on which standardization method was used). The results are shown in Figure 5, displaying linear climate responses to minimum temperatures, maximum temperatures and precipitation from February to August of the year of growth. Climate signals are relatively weak, and at best fairly marginal in their significance. Despite this, they were fairly consistent across the standardization models, although which parameters reached the arbitrary $p < 0.05$ significance threshold varied widely.

This exploratory analysis suggested two classes of climatic drivers of growth. The first, picked out by the ITA and IT models, is a June drought signal, where growth had a negative response to both June minimum and maximum temperatures. The second, detected by the ITA and TA models, was a positive response to late winter precipitation (February and March). The T model (raw chronology) could not detect either signal.

As a result of this exploratory analysis, as well as a priori suggestions from the literature, we selected winter precipitation, summer precipitation, June maximum temperatures, growing degree days, growing season length and water use efficiency as the predictor variables in the growth-climate models (see section 2.7 for further discussion). Figure 6 shows the time series of these predictor variables.

Using these six predictor models, both a linear and generalized additive model were fit to the log-transformed time effect of the ITA standardization model. The explanatory of these models was relatively low, but the generalized additive model (which assumes only smooth response) had a much better model fit (Table 4). The parameter estimates, uncertainty and p-values are shown in Table 5. Because two different models were fit, p-values for both models are reported as p-value for linear model / p-value for generalized additive model.

Winter precipitation had a positive, linear effect on growth ($p=0.04/p=0.19$), matching the results of the climate response analysis. Summer precipitation had a nonsignificant negative effect on growth ($p=0.16/p=0.08$), suggesting that it is either a weak influence or confounded by an omitted variable. June maximum temperature had a negative linear effect on growth ($p=0.08$ / $p=0.10$), as suggested by the response analysis. Growing degree days showed no effect at all in the linear model ($p=0.9997$) but a clear concave down effect in the generalized additive model ($p=0.05$). Growing season length had a positive influence on growth ($p=0.05$ / $p=0.09$). The linear model reported that

the effect of water use efficiency was weakly negative (p=0.15) but the generalized additive model told a more nuanced story, showing a concave down relationship (p=0.02).

4. Discussion

4.1 Presence of modern sample bias

Modern sample bias was clearly visible in the chronology. Productivity was strongly negatively correlated with age. As a result, long-term trends in forcing changed dramatically when tree-level productivity was accounted for. There is good reason to suspect the corrected approach is a better reflection of true historic patterns of tree growth. Model fit was much better and the climate signal was clearer after accounting for differences in productivity among trees.

Despite this, the origin of this bias is somewhat unclear. Big tree-selection bias (see [*Brienen et al.*, 2012b; *Cecile et al.*, in review]) should not be present under the sampling design followed. No minimum diameter cutoff was used and the stands were almost completely even-aged. There was a deliberate bias towards the selection of locally large, dominant trees, but this will not produce modern sample-bias when the largest trees are of the same age as the smallest.

The survivorship patterns of jack pine, locally, favour the fastest growing trees via competitive dominance due to their shade-intolerant nature [*Rudolph and Laidly*, 1990]. Yet this chronology showed a negative correlation between productivity and age; slow-growing trees were more likely to survive (or at least be sampled). In some studies, there may be sampling biases due to patchy resources, in which the stem density on fertile sites drops more rapidly than it does on less productive sites, effective reducing the relative survivorship of fast-growing trees [*Cecile et al.*, in review]. Yet this effect is unlikely here since a fixed number of trees were sampled from homogeneous sites and the stem density of the stands was irrelevant to their representation in the chronology.

Macro-scale disturbance biases may hold the answer however. The area around Silver Dollar, Ontario where this study occurred is actively managed. If disturbances affect large or productive trees, slow-growing trees will live longer, causing modern sample bias. Harvesting operations may be artificially biasing the stands selected for study. If a stand is highly productive, it is more likely to be logged (and thus wouldn't be sampled). If this was the case, only unproductive old stands would remain. This is a fairly plausible explanation for the modern sample bias observed in the chronology but one caveat remains. Trees are harvested only when it is economically viable to do so; they much reach a marketable size. As such, the signature of harvest-driven modern sample bias would show no relation between productivity and age at very young ages, and then the most productive stands would be gradually removed from the population. The trend seen here was a consistent decline, with no real flat unmarketable segment observed even for very young trees. Nevertheless, this is a fairly subtle signature and the sample here may not have been sufficiently large or robust to detect it. Harvest-driven survivorship bias remains the most plausible explanation of the observed modern sample bias.

4.2 Climate, growth and water use efficiency

The climatic drivers of jack pine growth have been extensively surveyed. Summer water limitation is cited in the negative response to summer temperature and growing degree days [*Hofgaard et al.*, 1999; *Larsen and MacDonald*, 1995] as well as water use efficiency [*Brooks et al.*, 2011; *Hoffer and Tardif*, 2009; *Savva et al.*, 2008; *Tardif and Conciatori*, 2001]. The positive effects of longer growing seasons [*Despland and Houle*, 1997; *Hofgaard et al.*, 1999; *Tardif and Conciatori*, 2001] were evident in our study, but the response to growing degree days was concave down, as might be expected due to the central location of the study sites within the jack pine range (compare to [*Botkin et al.*, 1991; *Despland and Houle*, 1997; *Hamel et al.*, 2004; *Hofgaard et al.*, 1999; *Huang et al.*, 2010; *Larsen and MacDonald*, 1995]).

This concave-down response to growing degree days has long been suggested by the agronomic and biogeographical literature [c.f. *Helmers*, 1962] and was used more than twenty years ago by *Botkin et al.* [1991] in dendrochronological analysis of jack pine. Intriguingly, the optimal growing degree days identified in that paper (~1500 GDD) using a naive quadratic estimate from range maps corresponds reasonably well to the optimum identified in this study (~1250 GDD) despite using completely different approaches. This raises the question of how common such concave and nonlinear climate responses are [*Loehle*, 2009]. Furthermore, it suggests, sensibly enough, that there may be a link between climate envelope models and climate response functions.

The relationship between growth and water use efficiency deserve special attention. Consistent with research in plant physiology, after a certain point water use efficiency was negatively associated with growth, suggesting that water use efficiency gains were likely driven by decreased stomatal conductance at the cost of photosynthesis [*Blum*, 2005]. But before that, water use efficiency had a positive influence on growth, suggesting true gains due to increased efficiency may be possible.

The climate-growth patterns identified were fairly tenuous but match well with both literature reports and ecological knowledge. Difficulties in standardization and climate interpolation both present difficulties in extracting a clear, reliable climate-growth relationship. Selecting appropriate functional forms for the climate response relationship remains challenging even with the use of generalized additive models, as predictor variables and interactions must still be specified. Simply looking at the correlation of climate variables to growth (or automated model selection processes) is prone to false positive inferences and can result in difficult to interpret or implausible models. The main bottleneck in dendrochronological climate-growth analysis remains the relatively short calibration period (limited by the length of the instrumental record). With only just over a hundred years to train the models, it is difficult to impossible to reliably investigate any but the strongest and least complex climate-growth dynamics.

4.3 Carbon fertilization

There was no clear, direct evidence for carbon fertilization in this study. Water use efficiency, expected to increase as CO_2 concentrations rise, is a mixed predictor of growth and appears to show drought stress rather than efficiency in many cases.

This, by and large, is consistent with the literature on the subject. Large scale reviews [*Boisvenue and Running*, 2006; *Gedalof and Berg*, 2010; *Peñuelas et al.*, 2011; *Silva and Anand*, 2012] show that any carbon fertilization effect that may occur is likely weak and that intrinsic water use efficiency is a poor predictor of the strength of these effects. *Girardin et al.* [2011] compared a process-based model to study the observed tree ring growth in jack pine. As in this study, they found that CO_2 fertilization was not necessary to explain the changes observed in growth.

The three major challenges facing those wanting to detect carbon dioxide fertilization using tree ring chronologies are as follows: First, long-term trends need to be appropriately reconstructed. Individual-series standardization is still widely used despite its long-known limitations for reconstructing long-term trends. Furthermore, modern sample bias may be a major problem when estimating trends longer than the lifespan of a single tree. Fortunately, as clearly demonstrated here, factor regression standardization can be used to address this bias.

Next, confounding climate variables must be controlled for. This is often challenging when only a relatively short (approximately 100 year) calibration period is available. However, process-based models and more sophisticated regression techniques such as the generalized additive models used here may help. An increase in growth as CO_2 levels rise does not necessarily imply that carbon fertilization is occurring.

Finally, more subtlety is needed in the search for the biological signature of carbon fertilization. The physiological literature makes specific predictions about the effect of carbon fertilization on water use efficiency: plants will become more drought tolerant and the trade-off between stomatal conductance and photosynthesis will be reduced. This combination should manifest in a shift in climatic optima. Drier, hotter weather will have less effect on tree growth and necessitate smaller increases in water use efficiency [*Soulé and Knapp*, 2006]. Future research needs to move beyond linear climate response models to look for these shifts, rather than focusing on simple increases in growth.

Carbon fertilization remains challenging to reliably detect from tree-ring data. With the use of fixed effects standardization, it is possible to reliably reconstruct long-term trends in tree growth, but there are further methodological difficulties. Investigators must correctly attribute changes in growth to changes in both climate and atmospheric CO_2, in the face of complex non-linear growth-climate links using only a century of calibration data. Further studies demand considerable sophistication, linking climate, growth and isotope data through process-based inquiries.

References

Ainsworth, E. A., and S. P. Long (2005), What have we learned from 15 years of free-air CO_2 enrichment (FACE)? A meta-analytic review of the responses of photosynthesis, canopy properties and plant production to rising CO_2, *New Phytologist*, *165*, 351–372.

Asshoff, R., G. Zotz, and C. Körner (2006), Growth and phenology of mature temperate forest trees in elevated CO_2, *Global Change Biology*, *12*(5), 848–861.

Barbour, M. M., T. J. Andrews, and G. D. Farquhar (2001), Correlations between oxygen isotope ratios of wood constituents of *Quercus* and *Pinus* samples from around the world,*Australian Journal of Plant Physiology*, *28*, 335–348.

Biondi, F., and K. Waikul (2004), DENDROCLIM2002: A C++ program for statistical calibration of climate signals in tree-ring chronologies, *Computers and Geosciences*, *30*(3), 303–311.

Blum, A. (2005), Drought resistance, water-use efficiency, and yield potential—are they compatible, dissonant, or mutually exclusive?, *Australian Journal of Agricultural Research*, *56*(11), 1159, doi:10.1071/AR05069.

Boisvenue, C., and S. W. Running (2006), Impacts of climate change on natural forest productivity evidence since the middle of the 20th century, *Global Change Biology*, *12*(5), 862–882.

Botkin, D. B., D. A. Woodby, and R. A. Nisbet (1991), Kirtland's Warbler habitats: a possible early indicator of climatic warming, *Biological Conservation*, *56*, 63–78.

Brewer, P. W., K. Sturgeon, L. Madar, and S. W. Manning (2010), A new approach to dendrochronological data management, *Dendrochronologia*, *28*(2), 131–134.

Brienen, R. J. W., E. Gloor, and P. A. Zuidema (2012a), Can we detect evidence for CO_2 fertilization from tree rings?, *Global Biogeochemical Cycles*, *26*, GB1025.

Brienen, R. J. W., E. Gloor, and P. A. Zuidema (2012b), Detecting evidence for CO_2 fertilization from tree ring studies: The potential role of sampling biases, *Global Biogeochemical Cycles*, *26*(1), GB1025, doi:10.1029/2011GB004143.

Briffa, K. R., Jones, P. D., Bartholin, T. S., Eckstein, D., Schweingruber, F. H., Karlen, W., Zetterberg, P., and Eronen, M. (1992). Fennoscandian summers from AD 500: temperature changes on short and long timescales, *Climate Dynamics*, *7*(3), 111-119.

Briffa, K. R., and T. M. Melvin (2011), A closer look at regional curve standardization of tree-ring records: justification of the need, a warning of some pitfalls, and suggested improvements in its application, in *Dendroclimatology*, vol. 11, edited by M. K. Hughes, T. W. Swetnam, and H. F. Diaz, pp. 113–145, Springer Netherlands.

Brooks, J. R., L. B Flanagan, and J. R Ehleringer (1998), Responses of boreal conifers to climate fluctuations: indications from tree-ring widths and carbon isotope analyses, *Canadian Journal of Forest Research*, *28*, 524-533.

Cecile, J., Pagnutti, C. and M. Anand (in review), A likelihood perspective on tree-ring standardization: eliminating modern sample bias.

Conroy, J., E. W. R. Barlow, and D. I. Bevege (1986), Response of Pinus radiata seedlings to carbon dioxide enrichment at different levels of water and phosphorus: growth, morphology and anatomy, *Annals of Botany*, *57*(2), 165–177.

Cook, E. R., K. R. Briffa, D. M. Meko, D. A. Graybill, and G. Funkhouser (1995), The "segment length curse" in long tree-ring chronology development for palaeoclimatic studies, *The Holocene*, *5*(2), 229–237, doi:10.1177/095968369500500211.

Despland, E., and G. Houle (1997), Climate influences on growth and reproduction of *Pinus banksiana* (Pinaceae) at the limit of the species distribution in eastern North America, *American Journal of Botany*, *84*(8), 928–937.

Dietze, M. C., and P. R. Moorcroft (2011), Tree mortality in the eastern and central United States: patterns and drivers, *Global Change Biology*, *17*, 3312–3326.

Duquesnay, A., N. Bréda, M. Stievenard, and J. L. Dupouey (1998), Changes of tree-ring δ13C and water-use efficiency of beech (*Fagus sylvatica* L.) in north-eastern France during the past century, *Plant, Cell & Environment*, *21*, 565–572.

D'Arrigo, R. D. (2004), Thresholds for warming-induced growth decline at elevational tree line in the Yukon Territory, Canada, *Global Biogeochemical Cycles*, *18*(3), GB3021, doi:10.1029/2004GB002249.

English, N. B., N. G. McDowell, C. D. Allen, and C. Mora (2011), The effects of Î±-cellulose extraction and blue-stain fungus on retrospective studies of carbon and oxygen isotope variation in live and dead trees, *Rapid Communications in Mass Spectrometry*, *25*(20), 3083–3090.

Etheridge, D. M., L. P. amd. L. Steele R.L., L. J. Francey, J.-M. Barnola, and V. I. Morgan (1998), Historical CO_2 records from the Law Dome DE08, DE08-2, and DSS ice cores, in *Trends: A Compendium of Data on Global Change*, Carbon Dioxide Information Analysis Center, Oak Ridge National Laboratory, U.S. Department of Energy, Oak Ridge, Tenn., U.S.A.

Farquhar, G. D., M. H. O'Leary, and J. A. Berry (1982), On the relationship between carbon isotope discrimination and the intercellular carbon dioxide concentration in leaves, *Functional Plant Biology*, *9*(2), 121–137.

Fritts, H. C. (1976), *Tree rings and climate*. Academic Press, London. 567 pp.

Gedalof, Z., and A. A. Berg (2010), Tree ring evidence for limited direct CO_2 fertilization of forests over the 20th century, *Global Biogeochemical Cycles*, *24*(3), 6.

Girardin, M. P., P. Y. Bernier, F. Raulier, J. C. Tardif, F. Conciatori, and X. J. Guo (2011), Testing for a CO_2 fertilization effect on growth of Canadian boreal forests, *Journal of Geophysical Research*, *116*.

Girardin, M. P., X. J. Guo, P. Y. Bernier, F. Raulier, and S. Gauthier (2012), Changes in growth of pristine boreal North American forests from 1950 to 2005 driven by landscape demographics and species traits, *Biogeosciences Discussions*, *9*(1), 1021–1053.

548 Graumlich, L. J., and L. B. Brubaker (1986), Reconstruction of annual temperature (1590-1979) for
549 Longmire, Washington, derived from tree Rings, *Quaternary Research*, *25*(2), 223–234.

550 Hamel, B., N. Bélanger, and D. Paré (2004), Productivity of black spruce and jack pine stands in
551 Quebec as related to climate, site biological features and soil properties, *Forest Ecology and*
552 *Management*, *191*(1–3), 239–251.

553 Helama, S., N. G. Makarenko, L. M. Karimova, O. A. Kruglun, M. Timonen, J. Holopainen, J. Merilainen,
554 and M. Eronen (2009), Dendroclimatic transfer functions revisited: Little Ice Age and Medieval
555 Warm Period summer temperatures reconstructed using artificial neural networks and linear
556 algorithms, *Annales geophysicae*, *27*(3), 1097–1111.

557 Helmers, H. (1962), Temperature effect on optimum tree growth. In *Tree Growth*, ed. T. T. Kozlowski.
558 Ronald Press, NY, pp. 275-87.

559 Hoffer, M., and J. C. Tardif (2009), False rings in jack pine and black spruce trees from eastern
560 Manitoba as indicators of dry summers, *Canadian Journal of Forest Research*, *39*(9), 1722–
561 1736, doi:10.1139/X09-088.

562 Hofgaard, A., J. Tardif, and Y. Bergeron (1999), Dendroclimatic response of *Picea mariana* and *Pinus*
563 *banksiana* along a latitudinal gradient in the eastern Canadian boreal forest, *Canadian Journal*
564 *of Forest Research*, *29*(9), 1333–1346.

565 Huang, J., J. C. Tardif, Y. Bergeron, B. Denneler, F. Beringer, and M. P. Girardin (2010), Radial growth
566 response of four dominant boreal tree species to climate along a latitudinal gradient in the
567 eastern Canadian boreal forest, *Global Change Biology*, *16*, 711–731.

568 Huang, J.-G., Y. Bergeron, B. Denneler, F. Berninger, and J. Tardif (2007), Response of forest trees to
569 increased atmospheric CO_2, *Critical Reviews in Plant Sciences*, *26*(5-6), 265–283.

570 Jacoby, G. C. (1997), Tree rings, carbon dioxide, and climatic change, *Proceedings of the National*
571 *Academy of Sciences*, *94*(16), 8350–8353, doi:10.1073/pnas.94.16.8350.

572 Körner, C., R. Asshoff, O. Bignucolo, S. Hättenschwiler, S. G. Keel, S. Peláez-Riedl, S. Pepin, R. T. W.
573 Siegwolf, and G. Zotz (2005), Carbon flux and growth in mature deciduous forest trees exposed
574 to elevated CO_2, *Science*, *309*(5739), 1360–1362.

575 LaMarche, V. C., D. A. Graybill, H. C. Fritts, and M. R. Rose (1984), Increasing atmospheric carbon
576 dioxide: tree ring evidence for growth enhancement in natural vegetation, *Science*, *225*(4666),
577 1019–1021.

578 Larsen, C. P. S., and G. M. MacDonald (1995), Relations between tree-ring widths, climate, and
579 annual area burned in the boreal forest of Alberta, *Canadian Journal of Forest Research*, *25*(11),
580 1746–1755, doi:10.1139/x95-189.

581 Leavitt, S. W. (2008), Tree-ring isotopic pooling without regard to mass: No difference from
582 averaging d13C values of each tree, *Chemical Geology*, *252*, 52–55.

583 Leavitt, S. W. (2010), Tree-ring C–H–O isotope variability and sampling, *Science of The Total*
584 *Environment*, *408*(22), 5244–5253.

Liñán, I. D., E. Gutiérrez, G. Helle, I. Heinrich, L. Andreu-Hayles, O. Planells, M. Leuenberger, C. Burger, and G. Schleser (2011), Pooled versus separate measurements of tree-ring stable isotopes, *Science of The Total Environment*, *409*, 2244–2251.

Loehle, C. (2009), A mathematical analysis of the divergence problem in dendroclimatology, *Climatic Change*, *94*(3-4), 233–245, doi:10.1007/s10584-008-9488-8.

McCarroll, D., and Loader, N. J. (2004), Stable isotopes in tree rings. *Quaternary Science Reviews*, *23*(7), 771-801.

McKenney, D. W., J. H. Pedlar, P. Papadopol, and M. F. Hutchinson (2006), The development of 1901–2000 historical monthly climate models for Canada and the United States, *Agricultural and Forest Meteorology*, *138*(1–4), 69–81.

Melvin, T. M., and Briffa, K. R. (2008), A "signal-free" approach to dendroclimatic standardisation, *Dendrochronologia*, *26*(2), 71-86.

Nelson, E. A. (2012), Climate change in the canadian boreal forest: the effect of warming, frost events, cloud cover and CO_2 fertilization on conifer tree rings, University of Toronto, PhD thesis.

Newman, J. A., M. H. Anand, H. A. L. Henry, and S. L. Hunt (2011), *Climate Change Biology*, CABI, 304 pp.

Ni, F., T. Cavazos, M. K. Hughes, A. C. Comrie, and G. Funkhouser (2002), Cool-season precipitation in the southwestern USA since AD 1000: comparison of linear and nonlinear techniques for reconstruction, *International Journal of Climatology*, *22*(13), 1645–1662, doi:10.1002/joc.804.

Norby, R. J., DeLucia, E. H., Gielen, B., Calfapietra, C., Giardina, C. P., King, J. S., ... & Oren, R (2005), Forest response to elevated CO_2 is conserved across a broad range of productivity, *Proceedings of the National Academy of Sciences of the United States of America*, *102*(50), 18052–18056.

Norby, R. J., and R. D. Zak (2011), Ecological lessons from free-air CO_2 enrichment (FACE) experiments, *Annual Review of Ecology, Evolution, and Systematics*, *42*, 181–203.

Peñuelas, J., J. G. Canadell, and R. Ogaya (2011), Increased water-use efficiency during the 20th century did not translate into enhanced tree growth, *Global Ecology and Biogeography*, *20*(4), 597–608.

Rudolph, T. D., and P. R. Laidly (1990), Pinus banksiana Lamb. jack pine, in R.M. Burns and B.H. Honkala (eds.), *Silvics of North America*, *Vol. 1, Conifers*, USDA Forest Service, Agricultural Handbook 654, Washington, DC. , 280-293

Savva, Y., Y. Bergeron, B. Denneler, A. Koubaa, and F. Tremblay (2008), Effects of interannual climate variations on radial growth of jack pine provenances in Petawawa, Ontario, *Canadian Journal of Forest Research*, *38*, 619–630.

Silva, L. C. R., and M. Anand (2012), Probing for the influence of atmospheric CO_2 and climate change on forest ecosystems across biomes, *Global Change Biology*, *22*(1), 83-92.

621 Soil Classification Working Group [SCWG] (1998), *The Canadian System of Soil Classification*,
622 Agriculture and Agri-Food Canada, Ottawa, Canada.

623 Soulé, P. T., and P. A. Knapp (2006), Radial growth rate increases in naturally occurring ponderosa
624 pine trees: a late-20th century CO_2 fertilization effect?, *New Phytologist*, *171*, 379–390.

625 Stewart, J. D., and J. Hoddinott (1993), Photosynthetic acclimation to elevated atmospheric carbon
626 dioxide and UV irradiation in *Pinus banksiana*, *PhysiologiaPlantarum*, *88*(3), 493–500.

627 Tardif, J., and F. Conciatori (2001), Comparative analysis of the climatic response of seven boreal
628 tree species from northwestern Quebec, Canada, *Tree-Ring Research*, *57*(2), 169–181.

629 Thomson, A. M., and Parker, W. H. (2008), Boreal forest provenance tests used to predict optimal
630 growth and response to climate change. 1. Jack pine, *Canadian Journal of Forest*
631 *Research*, *38*(1), 157-170.

632 Wood, S. N. (2006), *Generalized Additive Models: An Introduction with R*, Chapman &Hall/CRC, New
633 York, NY.

634

Tables

Model	n	k	σ	R^2	Adj. R^2	Δ AIC	Δ AICc	Δ BIC
G=ITA	18377	655	0.400	0.626	0.612	0	0	0
G=IT	18377	516	0.425	0.577	0.565	1963	1944	876
G=TA	18377	280	0.502	0.401	0.400	7655	7616	4723
G=T	18377	141	0.634	0.058	0.051	15945	15900	11926

Table 1: Model fit statistics for the competing tree ring width standardization models. See *Cecile et al.* [in press] for an explanation and discussion of the various model fit statistics in the context of tree ring standardization.

Individual effect	**G=ITA**	**G=IT**	**G=TA**	**G=T**
G=ITA	1	0.788	-	-
G=IT	0.788	1	-	-
G=TA	-	-	-	-
G=T	-	-	-	-
Time effect	**G=ITA**	**G=IT**	**G=TA**	**G=T**
G=ITA	1	0.164	0.787	0.329
G=IT	0.164	1	-0.448	0.484
G=TA	0.787	-0.448	1	0.068
G=T	0.329	0.484	0.068	1
Age effect	**G=ITA**	**G=IT**	**G=TA**	**G=T**
G=ITA	1	-	0.960	-
G=IT	-	-	-	-
G=TA	0.960	-	1	-
G=T	-	-	-	-

Table 2: Pearson correlations between the log-transformed estimated effects from the various tree ring width standardization models. Some combinations are missing as effects were not estimated by those models.

Model	n	k	σ	R^2	Adj. R^2	Δ AIC	Δ AICc	Δ BIC
G=ITA	1065	160.6	0.534	0.703	0.650	0	0	0
G=T	1065	135	0.730	0.443	0.362	618	600	491

Table 3: Model fit statistics for the two candidate water use efficiency standardization models. See *Cecile et al.* [in press] for an explanation and discussion of the various model fit statistics in the context of tree ring standardization.

Model	**n**	**k**	**Adj. R^2**	**Δ AIC**	**Δ BIC**
Linear	107	7	0.079	16.92	0
GAM	107	14.4	0.255	0	0.20

Table 4: Model fit statistics for the linear and generalized additive models (GAM) linking the growth time effect to the selected predictor variables.

Term	Linear model			GAM model		
	Estimate	**Std. error**	**p**	**Shape**	**Degrees of freedom**	**p**
Intercept	-6.187e-02	2.576e-01	0.8107	2.85e-2 ± 1.28e-2	1	0.0278
Winter precipitation	1.575e-03	7.581e-04	0.0403	Increasing	1.397	0.1900
Summer precipitation	-2.376e-04	1.700e-04	0.1652	Mixed	3.671	0.0847
June maximum temperature	-1.610e-02	9.055e-03	0.0784	Decreasing	1	0.1019
Growing degree days	4.257e-08	1.153e-04	0.9997	Concave down	2.525	0.0548
Growing season length	3.007e-03	1.573e-03	0.0588	Increasing	1	0.0875
Water use efficiency	-1.757e-04	1.206e-04	0.1484	Concave down	2.815	0.0208

Table 5: Regression coefficients, standard errors and significance for the parameters of the linear and generalized additive models (GAM) linking the growth time effect to the selected predictor variables. As a result of their flexible nature, GAM regression models do not have traditional parameters (such that could be listed in a table) or static standard errors. Instead, the shape and direction of the GAM effects are listed instead. Examining the partial predictions (Figure 7) of a generalized additive model is a much better way to understand the behaviour and certainty of each effect.

Figures

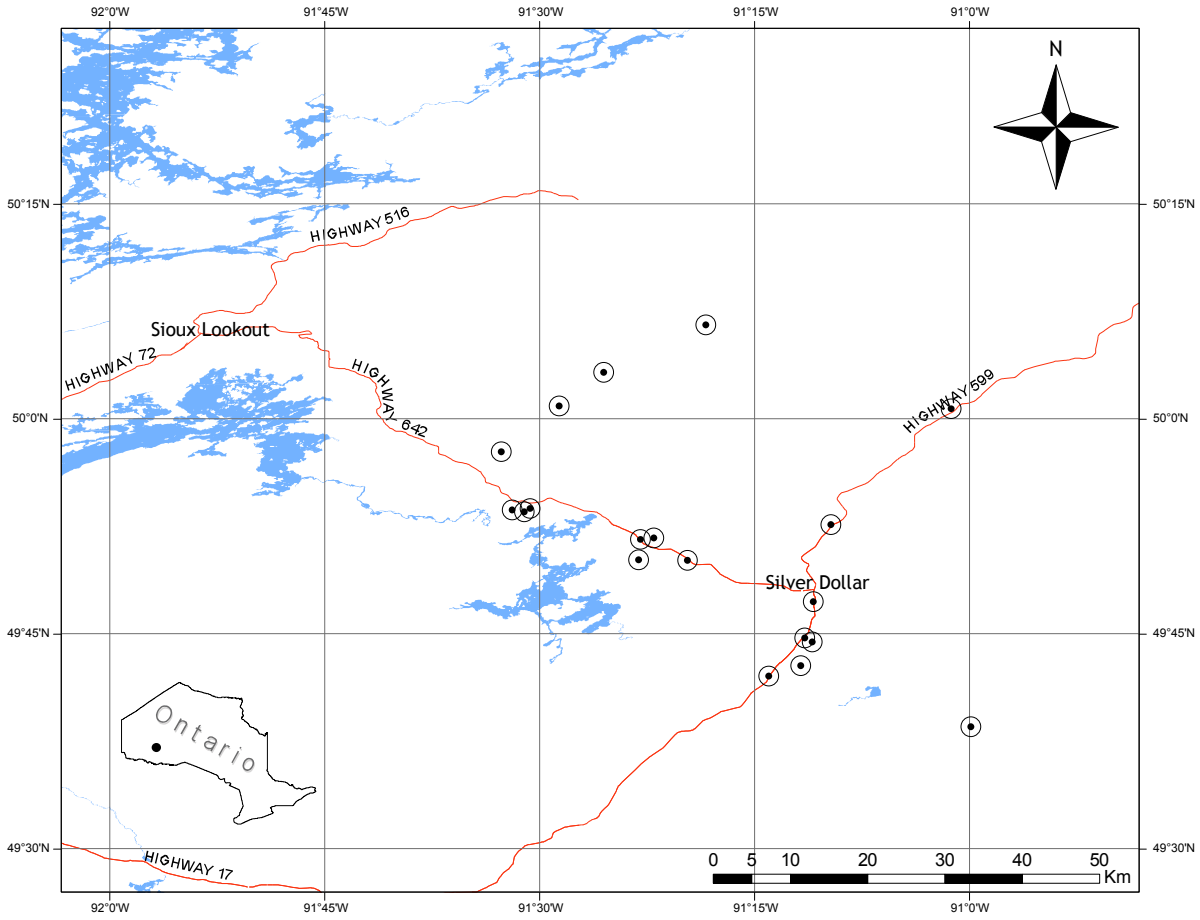

Figure 1: Location of jack pine stands used as study sites. See inset for location within Ontario.

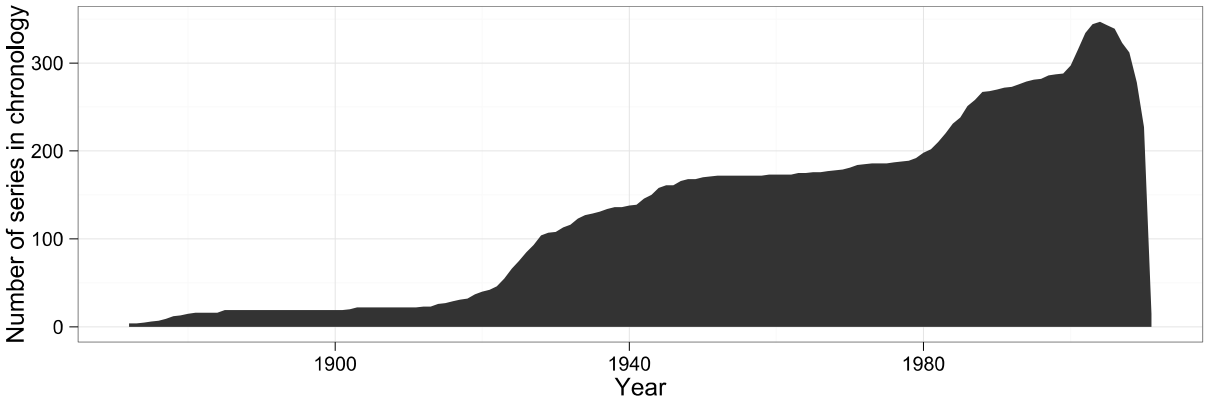

662
663 **Figure 2**: Number of series included in the chronology by year, indicating sample depth.

664

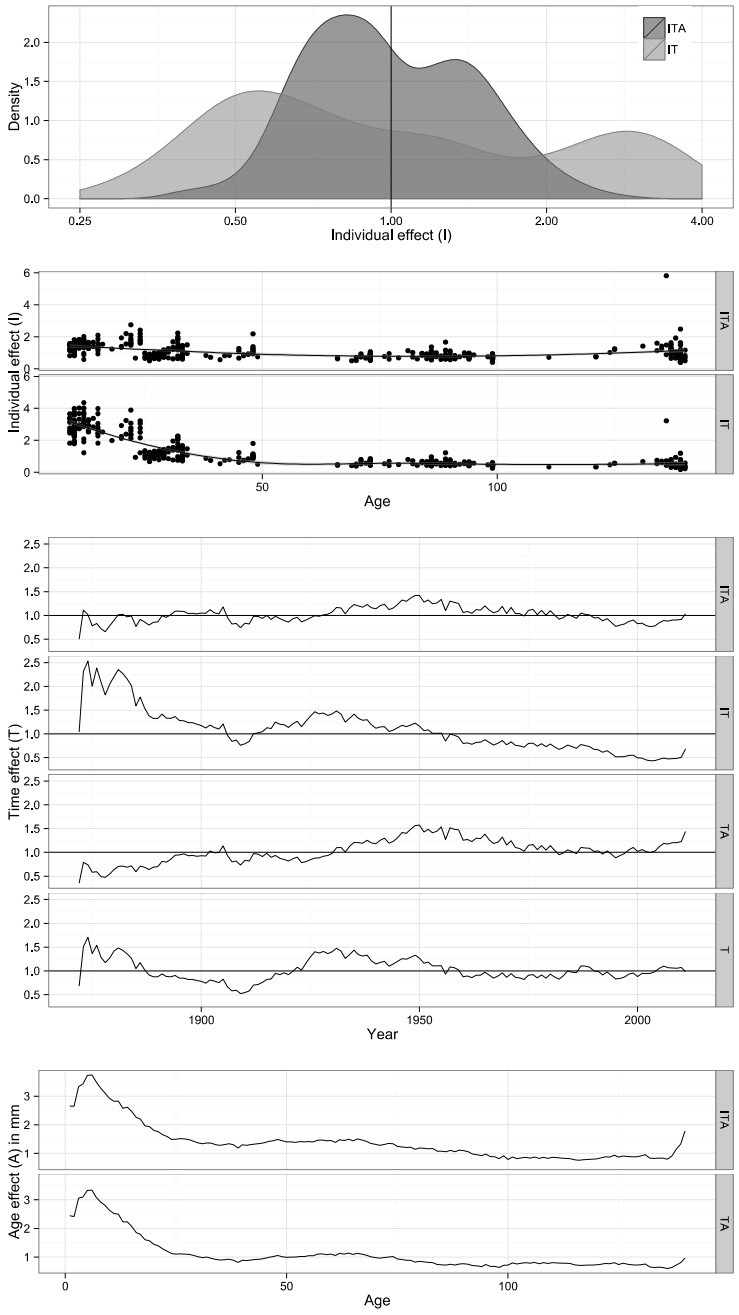

665

666

667

668 **Figure 3**: Effects estimated by various tree-ring standardization models for the jack pine ring width
669 chronology. The first two panels show the individual effect (**I**), first as a kernel density plot and then
670 as a scatter plot against age, with the smooth line indicating a loess-estimated trend. The third
671 panel shows the time effect (**T**) by year (analogous to the standardized chronology) as estimated by
672 each of the four competing standardization models. The fourth and final panel shows the age effect
673 (**A**) (completely unsmoothed) by cambial age and is roughly equivalent to the regional curve.

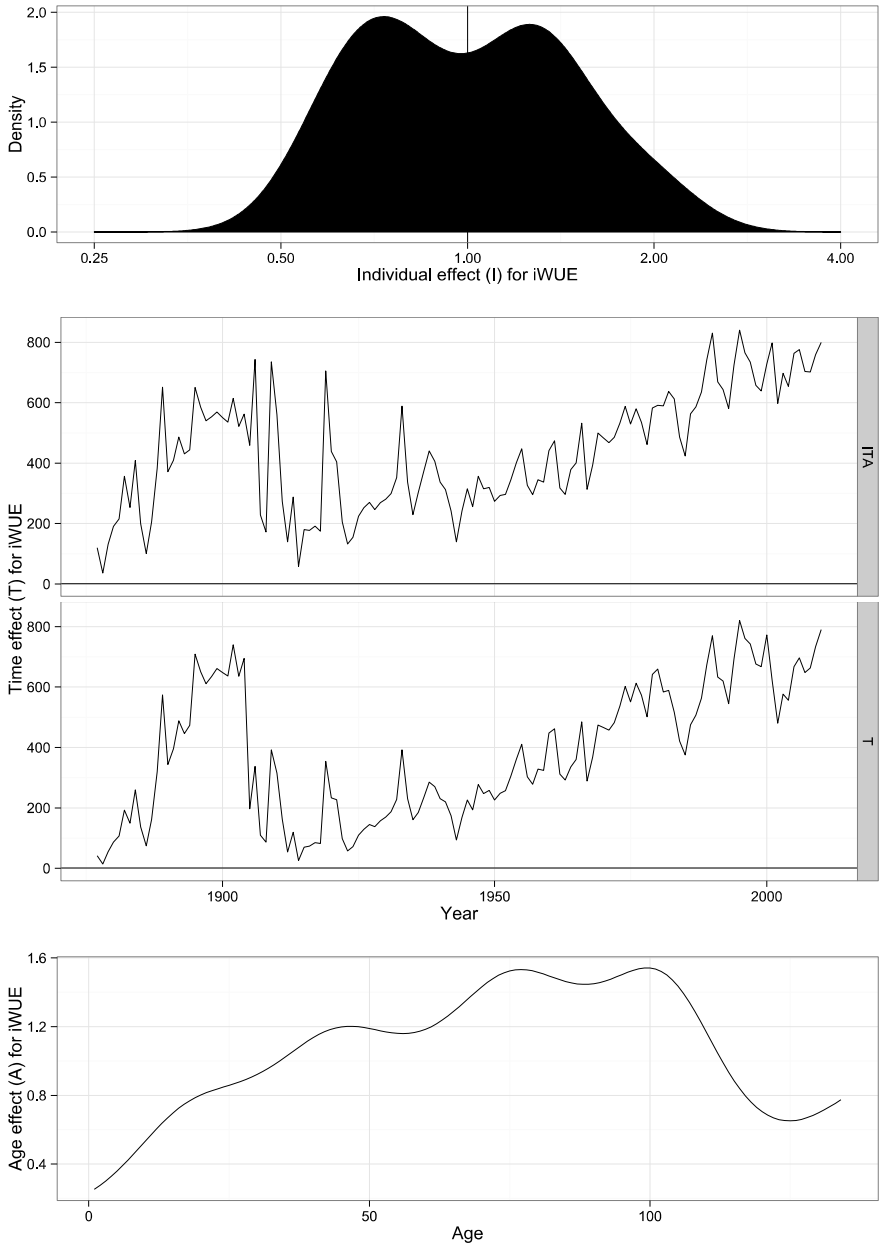

Figure 4: Effects estimated by various tree-ring standardization models for the jack pine water use efficiency chronology. The first panel shows a kernel density plot of site-level effects on water use efficiency (**I**). The second panel shows the time effect (**T**) of the "standardized" (ITA) and "raw" (T) water use efficiency chronology. The third and final panel shows the age effect (**A**) on water-use efficiency by stand age.

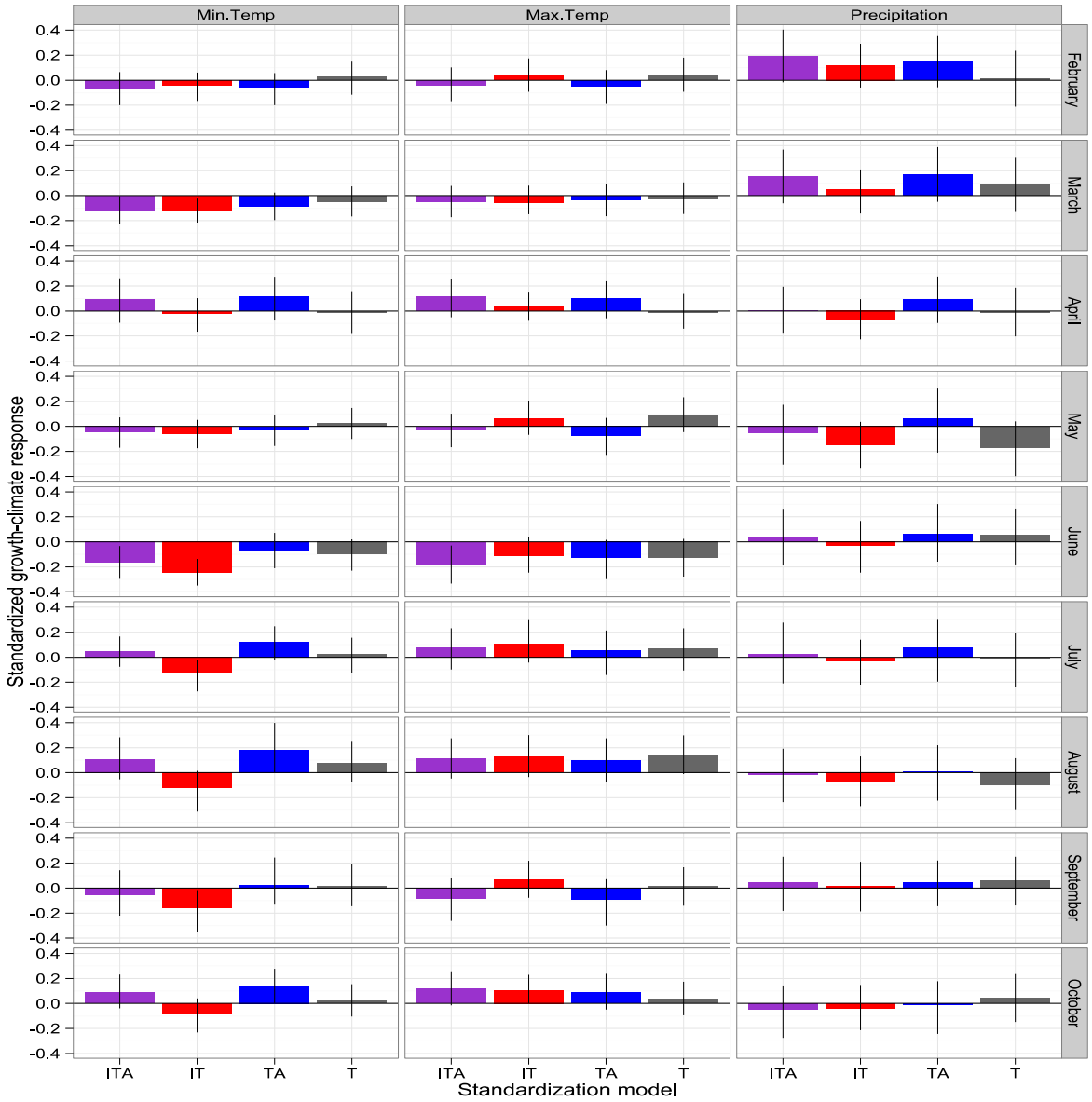

683

684 **Figure 5**: Bootstrapped linear climate responses (computed using the *bootRes* package in R [*Biondi*
685 *and Waikul*, 2004]) of the time effects from the four competing standardization models to monthly
686 climate data spanning 1901-2007. Error bars shown are 95% confidence intervals.

687

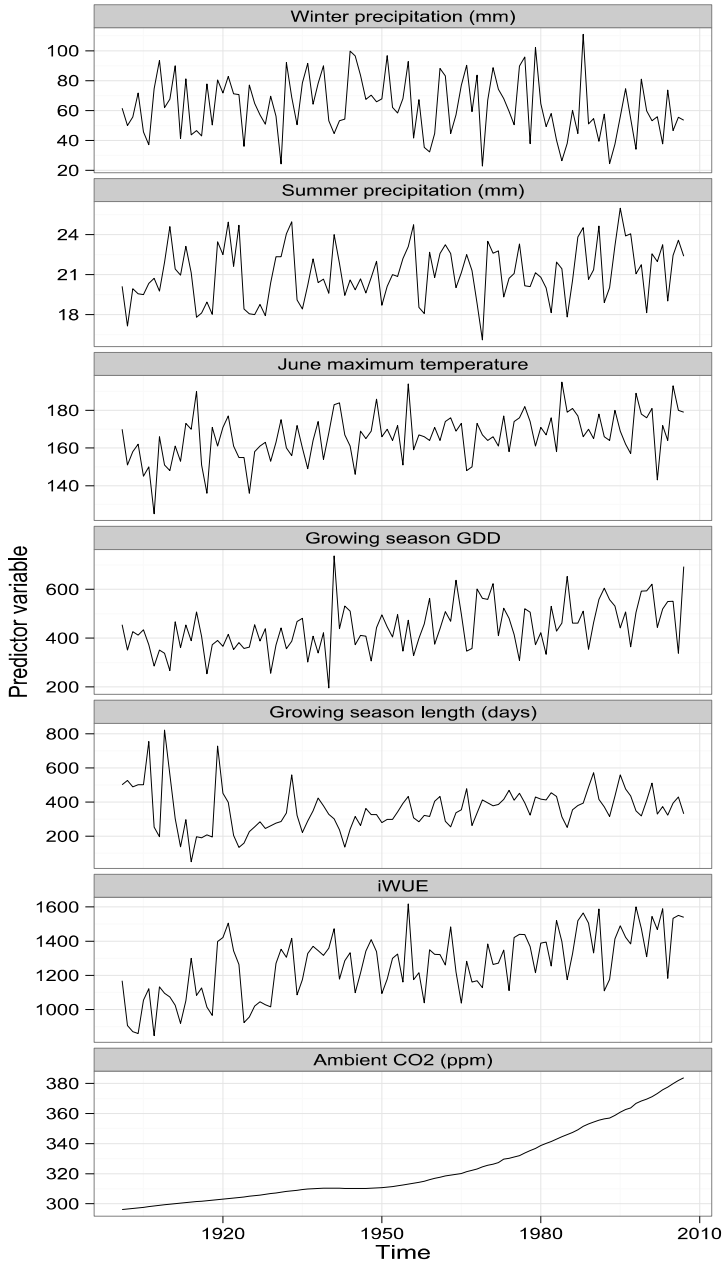

688 **Figure 6**: Time series of selected predictor variables from 1901 to 2007. The first five panels show
689 climatic and bioclimatic data interpolated from the instrumental record [*McKenney et al.* 2006]. The
690 sixth panel shows standardized water use efficiency derived from the $\delta^{13}C$ chronology collected
691 from the tree rings. The seventh, final panel shows the ambient level of atmospheric CO_2 for
692 comparison (it was not used as a predictor variable).

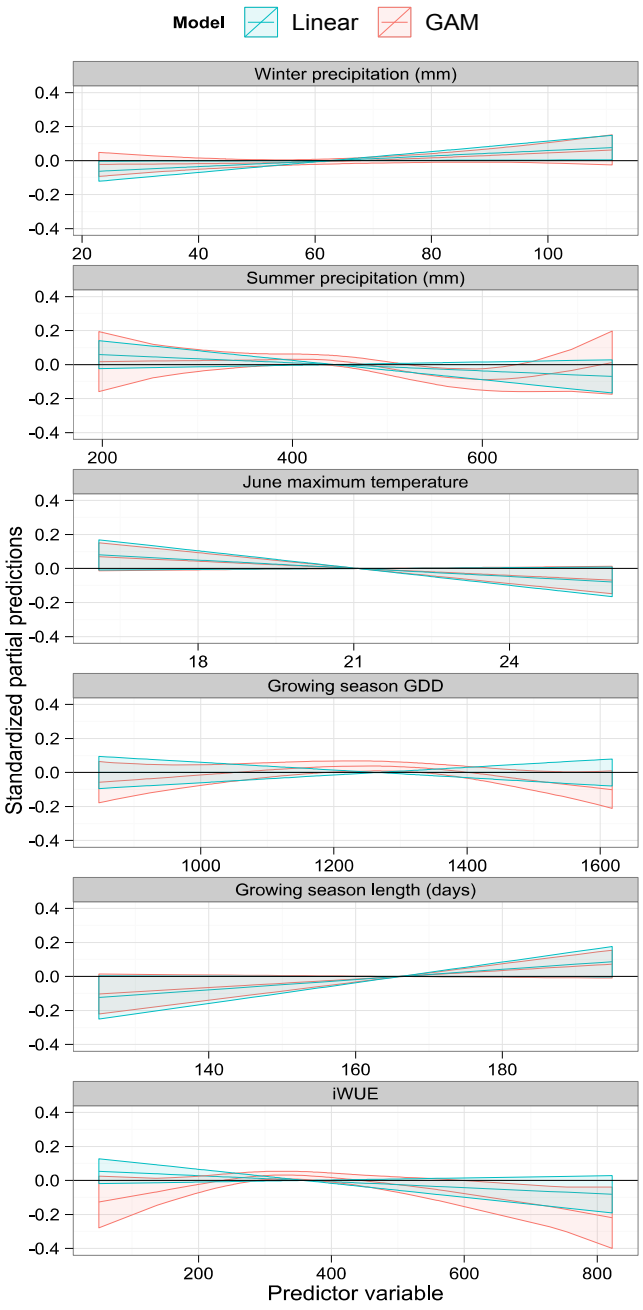

693

694 **Figure 7**: Partial predictions of the linear (blue) and generalized additive model (GAM, red)
695 regression fits of the time effect estimated by the ITA model to the selected predictor variables.
696 Ribbons shown denote 95% confidence intervals. The shape of the line shows the form and
697 direction of the response of growth to the predictor variables. The slope of the line can be directly
698 translated into linear regression coefficients. If the slope of the partial prediction for a particular
699 value of a predictor variable is positive, it means that an increase in that predictor variable would
700 result in increased growth (at least for a small increase).